J Mater Sci: Mater Med (2009) 20:563–572
DOI 10.1007/s10856-008-3596-x

Novel functionalized ternary copolymer fluorescent nanoparticles: synthesis, fluorescent characteristics and protein immobilization

Maolin Lu · Daocheng Wu · Na Guo

Received: 6 March 2008 / Accepted: 17 September 2008 / Published online: 7 October 2008

Abstract Novel fluorescent poly(styrene–acrylamide–acrylic acid) nanoparticles (FPSAAN) were synthesized by means of soapless emulsion polymerization and being modified with hydrazine hydrate by hydrazinolysis. The azidocarbonyl groups which can be rapidly coupled with proteins under mild condition were introduced onto the fluorescent nanoparticles by azido-reaction. Bovine serum albumin (BSA) was selected as a model protein to be covalently immobilized on the azidocarbonyl FPSAAN. Atom force microscopy (AFM), Transmission electron microscopy (TEM), Ultraviolet–visible (UV/Vis) spectrometer, Fourier transforms infrared spectrometer (FTIR), nanoparticle size analyzer and fluorescence spectrophotometer were used to characterize the FPSAAN. Results showed that FPSAAN had a regular spherical shape, and a dramatic narrow size distribution (polydispersity index 0.046 ± 0.009). The fluorescence intensity of FPSAAN ($\lambda_{ex}/\lambda_{em} = 253/306$ nm), hydrazide-FPSAAN ($\lambda_{ex}/\lambda_{em} = 260/326$ nm), and protein-immobilized FPSAAN ($\lambda_{ex}/\lambda_{em} = 258/325$ nm) was linearly related to the concentration ranging from 1.0×10^{-3} g l^{-1} to 10.0×10^{-3} g l^{-1}. The linear relationship was obtained. The equations are $y = 52.808x + 16.465$ ($R^2 = 0.9927$), $y = 5.1814x + 4.1535$ ($R^2 = 0.9935$) and $y = 5.2227x + 5.2883$ ($R^2 = 0.9937$), respectively. In addition, external factors such as pH and ionic strength exert a slight influence on fluorescent properties. The experiments of the immobilization of BSA indicated that FPSAAN with azidocarbonyl groups could be covalently coupled with BSA at the rate of 41.1%. Meanwhile, hCG antibody immobilized FPSAAN have the similar fluorescence characteristics to BSA immobilized FPSAAN. Only negligible difference of the fluorescence characteristics can be found. Furthermore, the fluorescence characteristics of hCG antibody immobilized FPSAAN have not been obviously affected after mixed with the hCG antigen and human plasma. These novel azidocarbonyl FPSAAN with stable fluorescence and active functional azidocarbonyl groups could be used as a promising fluorescent probe for quantitative detection, protein immobilization, cell labeling research and early rapid clinical diagnostics.

Abbreviations

PSAAN	Poly(styrene–acrylamide–acrylic acid) nanoparticles
FPSAAN	Fluorescent poly(styrene–acrylamide–acrylic acid) nanoparticles
Hydrazide-FPSAAN	FPSAAN bearing hydrazide groups
Azidocarbonyl FPSAAN	FPSAAN bearing azidocarbonyl groups
Protein-immobilized FPSAAN	Azidocarbonyl FPSAAN coupling with BSA

1 Introduction

Recently, nanoparticles have been widely used in biomedical fields such as bioseparation [1, 2], immunoassay [3, 4], assessing protein [5], and controlled release [6], owing to their unique characteristics of large specific surface area,

M. Lu · D. Wu (✉) · N. Guo
The Key Laboratory of Biomedical Information Engineering of Ministry of Education, School of Life Science & Technology, Xi'an Jiaotong University, Xi'an 710049, People's Republic of China
e-mail: wudaocheng@mail.xjtu.edu.cn

homogeneous size, stability and capability of coupling with biological activated materials. Among various nanoparticles, fluorescent nanoparticles have attracted great attention in various fields, such as cell labeling [7–10], investigation of molecular interactions [11], drug deliver [12], and deoxyribonucleic acid (DNA) hybridization [13], since they not only offer sensitive detection by analysis of their fluorescent properties, but also are expected to be more flexible in immunolabeling. Additionally, these fluorescent nanoparticles possess high brightness and improved photostability compared to conventional fluorescent dyes.

Fluorescent nanoparticles currently available include colloidal inorganic semiconductor quantum dots [14], dye-loaded latex spheres [15] and dye-doped silica colloids [16]. For the dye-loaded silica colloids, limited dye-loading concentration due to self-quenching is a critical problem [17]. Semiconductor quantum dots recently developed as a new class of fluorescent markers has sparked intense excitement in the fields of biology and medicine due to their higher sensitivity and better photostability [18]. However the deficiencies such as high price, difficult combination with other macromolecules and no functional groups existing on the surface limit the wide application in practice.

To overcome these obstacles, we attempt to develop novel fluorescent nanoparticles with low-cost fluorescent reporter and active surface functional groups, which may offer the opportunities to easier combine with macromolecules and less expensive in production. Sensitive fluorescent characteristics and low price of fluorescein [19] make it an excellent candidate as fluorescence reporter in our work (Fig. 1). However, it also has shortcomings of inferior life-span and insufficient photochemical stability. The critical challenge of using fluorescein is whether fluorescein can be firmly embedded. If fluorescein can be successfully embedded into nanoparticles, the nanoparticle matrix can protect the embedded fluorophores from quenching agents, photobleaching, solvent polarity, pH, and ionic strength, thus stabilize the fluorescence emission signal that further contribute to the life-span and photochemical stability [20]. In addition, surface functional groups on the nanoparticles are necessary for conjugation with proteins, nucleic acids, or low-molecular-weight compounds. Currently, surface groups of the nanoparticles such as aldehyde, carboxyl and amino groups are often synthesized and used as supports [21–23]. It has been well known that the aldehyde groups are unstable and the carboxyl groups have low binding capacity with proteins. Amino groups have merits derived from their high stability and reactivity, which contribute to their wide applications as active surface functional groups. But the nanoparticles with quantity of amino groups are difficult to be obtained. Furthermore, from the standpoint of protein immobilization, they often need to be activated via cross-linking agents before they can covalently link to

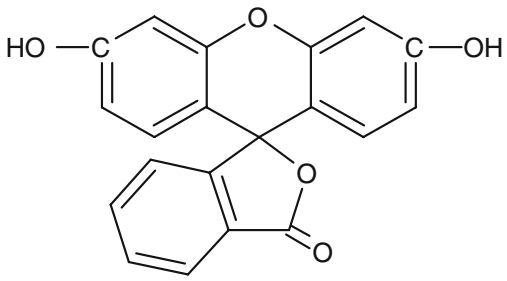

Fig. 1 The chemical structure of fluorescein

proteins [24]. And this method is comparative laborious and expensive. Liu et al. [25] has described the preparation of diazotized polystyrene latex (the active diazo groups on diazotized polystyrene latex could be covalently coupled with phenol and imidazole groups of antibodies via a covalent bond linkage without any cross-linking agent). This method of protein immobilization is rapid with high specificity, and the conjugation with antibody protein is firm with 20–40% binding capacity. However, the preparation of diazotized polystyrene latex is complicated and laborious with several steps (emulsion polymerization, nitration, reduction and diazotization) and the process is difficulty to control.

In our experiments, the monomer acrylamide (AAM) was introduced into polymerization process and FPSAAN with amine groups were synthesized by a two-step simple polymerization reaction. Subsequently surface modifications were performed comprising hydrazinolysing amide groups on the FPSAAN to hydrazide groups and diazotizing carboxylic hydrazide groups formed on the FPSAAN to azidocarbonyl groups. Finally, chemical coupling between BSA and the latex takes place by a displacement reaction of the protein's amino groups onto the latex polymer's surface azidocarbonyl groups. The reaction sequence is illustrated in the Scheme 1, and the processes are simple, rapid and easy to control with low cost. Cumulative results of fluorescence measurements, FTIR spectra, and high entrapment efficiency of fluorescein in FPSAAN along with the superior solubilization as well as strict stability of the FPSAAN indicate that fluorescein has been embedded into the nanoparticles and FPSAAN own superior fluorescent characteristics. Remarkably, the quantitative experiment demonstrates a superior linear relationship between protein-immobilized FPSAAN concentrations and the fluorescence intensity. Moreover, the experiments of the immobilization of proteins show that the amount of BSA covalently immobilized is over 41%. Meanwhile, the fluorescence characteristics of hCG antibody immobilized FPSAAN almost remain the same after mixed with the hCG antigen and human plasma, respectively. The application of the fluorescent nanoparticles with surface azidocarbonyl groups is promising to provide a new

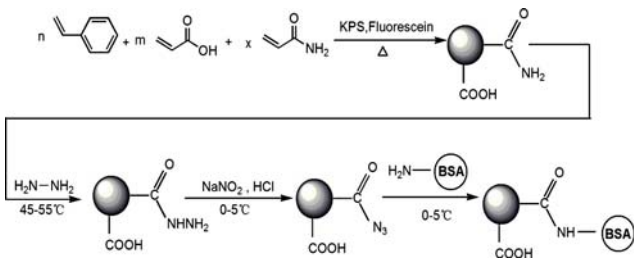

Scheme 1 The schematic diagram of the fabrications of FPSAAN, hydrazide-FPSAAN, azidocarbonyl FPSAAN and protein-immobilized FPSAAN

reagent for early and rapid clinical diagnostics, immunological studies and quantitative detection in the future.

2 Materials and methods

2.1 Materials

Styrene (St, chemically pure, Chinese Medical Chemicals Company Limited, Shanghai, China) was distilled under reduced pressure to remove the inhibitor. Other chemicals such as acrylamide (AAM, analytical reagent, Amresco Fraction, America), acrylic acid (AA, analytical reagent, Third Chemical Plant, Tianjin, China), potassium persulfate (KPS, analytical reagent, Chemical Plant, Xi'an, China), sodium dodecylsulfate (SDS, analytical reagent, Sanland Chemicals Company Limited, Xiamen, China), Fluorescein(analytical reagent, Chemical Reagent Corporation, Shanghai, China), bovine serum albumin (BSA, Mr 68000, Roche Fraction, Germany), were of analytical grade obtained commercially and used without further purification. Human chorionic gonadotropin (hCG) antibody (2.0 mg ml^{-1}) and human chorionic gonadotropin (hCG, 1.0 μg ml^{-1}) were provided by Zhengzhou Autobio Co. Ltd of China.

2.2 Synthesis

2.2.1 Synthesis of FPSAAN

FPSAAN were prepared by soapless emulsion polymerization carried out in a three-necked separator flask, equipped with a stirrer, a spiral condenser, and a dropping funnel with a nitrogen inlet. Double distilled water was boiled firstly in order to remove oxygen. Briefly, fluorescein (0.05 g) was mixed with acrylamide (3.80 g), then the mixture was added into the three-necked separator flask with 170 ml double distilled water, the mixture was heated up to 45°C under stirring, afterward, styrene (16.00 g) was introduced into three-necked separator flask dropwise. The polymerization was allowed to proceed at 80°C for 3 h in still N_2 atmosphere after adding KPS (0.40 g) and acrylic acid (0.20 g). The production was purified by dialysis three times with distilled water, and then filtered through filter (2 mm) paper. Finally, it was lyophilized to primrose yellow powder and stored at 4°C before use.

2.2.2 Synthesis of hydrazide-FPSAAN and azidocarbonyl FPSAAN

The modification of surface functional groups on the homogeneous fluorescent nanoparticles as described in this section was done analogous to the described method [26], comprising a two-step reaction sequence.

In the first step, fluorescent nanoparticles bearing the hydrazide groups on the surface, called as hydrazide-FPSAAN, were fabricated by hydrazinolysis. In brief, FPSAAN (20 ml, 5%) were added into a flask with the volume of 50 ml under continuous magnetic stirring. The hydrazide reaction was allowed to proceed at 45°C for 8 h, followed by the addition of excess hydrazine hydrate (80%). After cooled to the room temperature, the production was purified by dialyzing hydrazide-FPSAAN for several times, which is sufficient to remove unreacted hydrazine using distilled water.

In the second step, functional azidocarbonyl fluorescent nanoparticles (azidocarbonyl FPSAAN) were prepared by the azido-reaction. Briefly, the pH of a certain volume of hydrazide-FPSAAN suspension (5%, 5.0 ml) was adjusted to 1–2 with 1.0 mol l^{-1} HCl solution under magnetic stirring, and then 0.1 mol l^{-1} $NaNO_2$ solution was added dropwise into the suspension till the color of starch KI indicator paper changed within a period of about one minute. The reaction was stirred at 0–5°C for 1 h. Further purification was carried out at 4°C.

2.2.3 Synthesis of protein-immobilized FPSAAN

BSA was selected as a model protein to test the immobilization characteristics of functional azidocarbonyl FPSAAN. First of all, 2.5 ml freshly azidocarbonyl FPSAAN was added into a reactor. The pH was adjusted to 8.0 with 1.0 mol l^{-1} NaOH solution at 0–5°C under magnetic stirring. BSA (70 μl, 10%, pH 8.0) was diluted by slowly adding PBS buffer solution (8.0, 1/15 mol l^{-1}) into the reactor. Then the system was stirred at 0–5°C for 5 h. Glycine (1.0 ml, 2.5%, pH 8.0) was added to discharge unchanged azidocarbonyl groups, and then the mixture was dialyzed by double distilled water to wash away salt, ion and other small molecules materials. Finally, the final product was centrifuged under 20,000 rpm and the supernatants were collected for analysis of BSA concentration. Meanwhile, the hCG antibody was also immobilized on azidocarbonyl FPSAAN according to the same process as described above.

2.3 Particle size and morphology of FPSAAN

The morphology of FPSAAN was examined by Transmission electron microscopy (JEM-2000 EX, Hitachi, Japan). In order to verify the result of TEM, the morphology of FPSAAN was also assessed using an Atom force microscopy (AFM, NTEGRA Prima, Russia). The average diameter and polydispersity index of FPSAAN, hydrazide-FPSAAN and protein-immobilized FPSAAN were measured by photon correlation spectroscopy (PCS) (Malvern zetasizer Nano ZS90, Malvern instruments Ltd., UK) with a 50 mV laser. Typically, appropriate concentrations of these nanoparticles were diluted, respectively, by 1 ml of water before adding into the sample cell. The measurement time was set at 2 min (rapid measurement) and each run consisted of 10 subruns. Each value reported was the average of at least three measurements.

2.4 Functional groups on the surface of FPSAAN

The functional groups on the surface of FPSAAN were evaluated by a Fourier transform infrared spectrometer (FTIR, IRpresitge-21, Japan) by using KBr pellets. To contrast, the FTIR spectra of fluorescein and PSAAN were also recorded.

2.5 Fluorescence spectrum

Fluorescein solution, FPSAAN, freshly hydrazide-FPSAAN and protein-immobilized FPSAAN aqueous solutions were estimated to prove the potential of functionalized nanoparticles by the measurement of fluorescence spectroscopy using a fluorescence spectrophotometer (F-2500, Hitachi, Japan) at the room temperature. The emission and excitation slit widths were 5.0 and 5.0 nm, respectively. The scan speed was fixed at 300 nm per min.

2.6 Immobilization of protein

The immobilization capacity of BSA was determined by ultraviolet spectrophotometer (ultrospec 2100 pro, Amersham Biosciences, Sweden). The total unbound BSA collected in all supernatants was measured according to a calibration curve. The amount of BSA immobilized on the functional azidocarbonyl-FPSAAN was then determined by measuring the initial and unbound concentrations of BSA. The experiment was repeated for three times.

2.7 Influence of the hCG antigen and plasma

About 20 μl of hCG antigen as well as 20 μl of human plasma was added to 1.0 ml hCG antibody immobilized FPSAAN, respectively. In order to evaluate the possible changes of fluorescence, we measured the fluorescent characteristics before and after the hCG antigen and human plasma were added.

3 Results and discussion

3.1 Characterization of FPSAAN

3.1.1 The particle morphologies and size distribution

TEM and ATM images of FPSAAN are presented in Fig. 2a and b, respectively, which demonstrate the similar regular spheres of a narrow particle size distribution with similar size about 200–210 nm. Both techniques confirmed that the FPSAAN were circular in shape, well dispersed

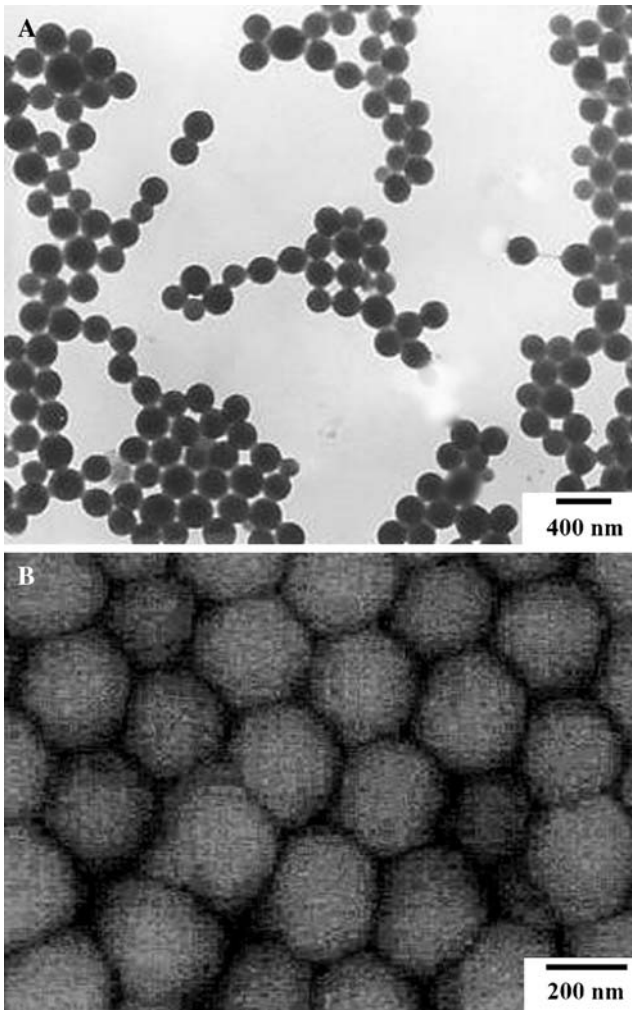

Fig. 2 Particle morphologies of FPSAAN: **a** TEM and **b** ATM images

Table 1 Particle size, and polydispersity index (PDI) of FPSAAN, hydrazide-FPSAAN and protein-immobilized FPSAAN ($n = 3$)

Sample title	Size (nm)	PDI
FPSAAN	258.2 ± 1.9	0.046 ± 0.009
Hydrazide-FPSAAN	253.3 ± 5.5	0.073 ± 0.04
Protein-immobilized FPSAAN	282.6 ± 5.4	0.044 ± 0.028

and separated on the surface. Table 1 showed the average diameter being 258.2 ± 1.9 nm for FPSAAN, with a very narrow distribution (polydispersity index 0.046 ± 0.009).

The discrepancy in the size of the same FPSAAN in the Fig. 2 and Table 1 was due to the fact that the dynamic light scattering method gave the hydrodynamic diameter rather than the actual diameter of FPSAAN. In fact, the mean diameter measured using TEM was significantly smaller than that obtained with the dynamic light scattering method. The size detection of FPSAAN by PCS was carried out in aqueous state where lipid nanospheres were highly hydrated, causing the diameters detected by PCS were 'hydrated diameters'—larger than their genuine diameters. However, PCS does not 'measure' particle sizes [27]. The particle size was further validated by the TEM of the FPSAAN.

Additionally, Table 1 also showed some information about the size distribution, and polydispersity index of hydrazide-FPSAAN and protein-immobilized FPSAAN, which indicates the average diameter being 253.3 ± 5.5 nm for hydrazide-FPSAAN and 282.63 ± 5.4 nm for protein-immobilized FPSAAN along with a very narrow distribution (polydispersity index: 0.073 ± 0.04 and 0.044 ± 0.028, respectively). Remarkably, further assays (data not shown) demonstrated that the particle size of the particles at different degree of pH, salt concentration, and aging time, as a whole, illustrated no apparently altered trending, respectively.

3.1.2 Entrapment efficiency, water solubility and stability

FPSAAN prepared in this study are an aqueous colloidal dispersion of water-soluble nano-sized particles. The loading capacity of FPSAAN is found to be satisfactorily high, with entrapment efficiency (EE) being 85%, which was calculated using the following Eq. 1:

$$\mathrm{EE}\ (\%) = \frac{\text{amount of fluorescein added} - \text{amount of fluorescein isolated}}{\text{amount of fluorescein added}} \times 100\% \quad (1)$$

Additionally, there are no deposited particles and no aggregation occurring in the aqueous colloidal system within more than two years stored at 4°C. The superior solubility and dramatic stability may be attributed to the particular coupling patterns of fluorescein-polymer, which is that fluorescein may be covalently linked to the polymer when be physically incorporated. The remarkable stabilization can contribute to the better suitability for instrumental diagnosis based on the absorption or transmission of light in biomedical fields.

3.1.3 FTIR spectrum

The FTIR spectra are shown in Fig. 3, including poly(styrene–acrylamide–acrylic acid) nanoparticles (PSAAN), FPSAAN and fluorescein. In the FTIR spectrum of PSAAN (Fig. 3a), characteristic absorption peaks of benzene ring appear, the wide peak at 3462 cm^{-1} is assigned to the superimposed stretching vibrations of O–H and N–H bonds, and the strong peak at 1652 cm^{-1} is attributed to the C=O bond vibration, which confirm the presence of carboxyl groups and amino groups. Thus, obvious characteristic signals for both amide groups and benzene ring groups imply that both acrylamide and styrene have participated in polymerization reaction. In the FTIR spectrum of fluorescein (Fig. 3c), the present of carbonyl groups and unique benzene ring are confirmed by characteristic peaks at 1647 and 756 cm^{-1}, respectively. Figure 3b represents the FTIR spectrum of FPSAAN, which compared with what illustrated in Fig. 3a shows new bands at 1647 and 756 cm^{-1} that were also appeared in Fig. 3c, indicating qualitatively the overall presence of amide and fluorescein in the FPSAAN.

3.2 Fluorescent characteristics

The fluorescence spectra of FPSAAN, hydrazide-FPSAAN and protein-immobilized FPSAAN (5.0 mg l^{-1}) are presented in Fig. 4, respectively. It is shown that FPSAAN, hydrazide-FPSAAN and protein-immobilized FPSAAN can give off fluorescence. The maximum excitation and emission wavelengths are as follows:

Fluorescein $\lambda_{ex}/\lambda_{em} = 489/513$ nm;
FPSAAN $\lambda_{ex}/\lambda_{em} = 253/306$ nm;
Hydrazide-FPSAAN $\lambda_{ex}/\lambda_{em} = 260/326$ nm;
Protein-immobilized FPSAAN $\lambda_{ex}/\lambda_{em} = 258/325$ nm.

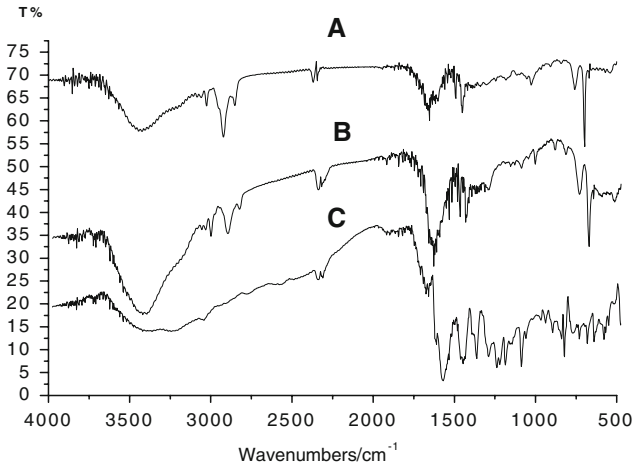

Fig. 3 FTIR spectra of A PSAAN, B FPSAAN and C fluorescein

The observed discrepancy of fluorescence intensity and the notable blue shift of fluorescein in nanoparticles indicate that fluorescein has been incorporated into the polymer network. The discrepancies of different nanoparticles' fluorescence spectra and the fluorescence intensity are generally attributed to the classical light-scattering effects and different radiative transitions, in this case the molecules strongly differing in the distribution of valence electrons which might have an effect on the fluorescent properties. However, the present data-obtained under the strictly controlled conditions-suggest that these discrepancies for the different nanoparticles are probably attributable to the surface groups.

The finely fluorescent characteristics are advantages of using these functionalized FPSAAN as diagnostic agents. According to our study, the PSAAN have associated with a fluorescent tracer material (fluorescein). When it is stimulated by the absorption of incident radiation, the functionalized FPSAAN can emit fluorescence persistently as long as the stimulating radiation is continued. As a result, by means of analysis of its fluorescent properties characterized by the fluorescence spectroscopy, functionalized FPSAAN can achieve optical coding as a marker to recognize the category of samples.

3.2.1 The effect of pH

The effects of pH of fluorescein, FPSAAN, hydrazide-FPSAAN and protein- immobilized FPSAAN on fluorescent characteristics discussed are illustrated in Fig. 5. In Fig. 5a, the fluorescence intensity of fluorescein shows a dramatic transformation (pH 6.0) showing the instability of

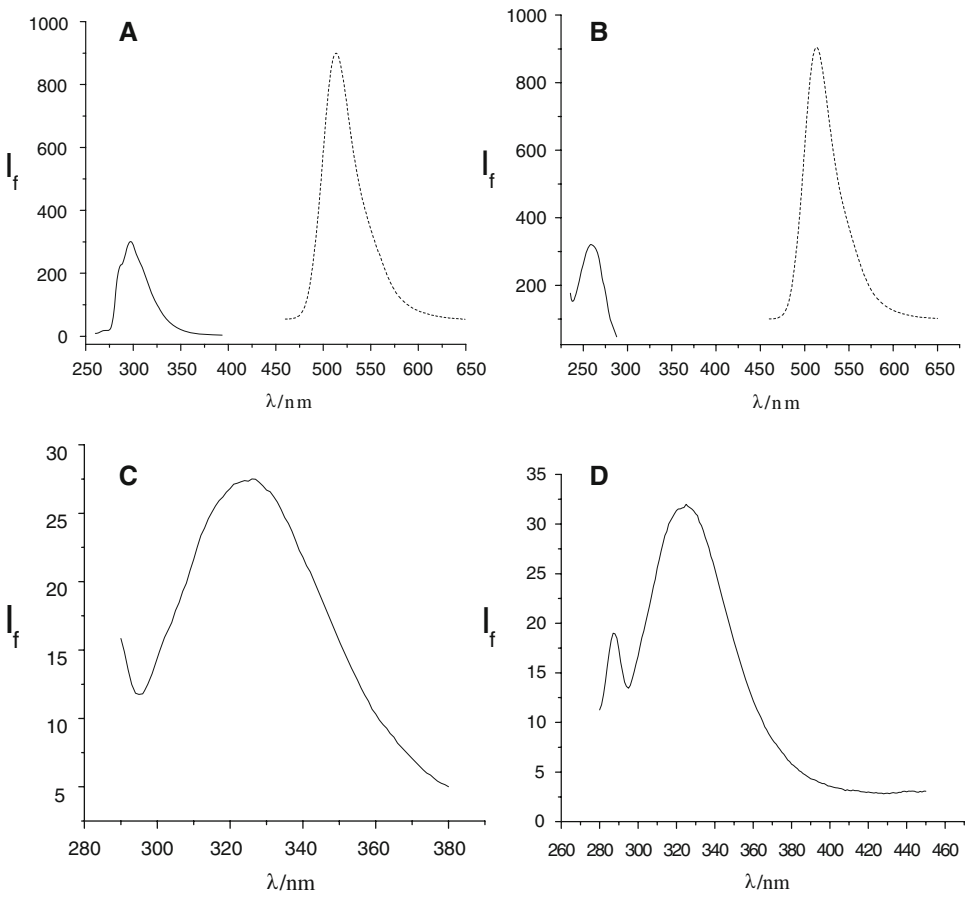

Fig. 4 Fluorescence spectra of FPSAAN, fluorescein, hydrazine-FPSAAN and protein-immobilized FPSAAN aqueous solution: **a** emission spectra of fluorescein excited at 489 nm (dash line) and FPSAAN excited at 253 nm (solid line), **b** excitation spectra of fluorescein (dash line) and FPSAAN (solid line), **c** emission spectrum of hydrazide-FPSAAN excited at 260 nm, and **d** emission spectrum of protein-immobilized FPSAAN excited at 258 nm. The "I_f" here symbolizes the fluorescence intensity

pure fluorescein. In Fig. 5b, it is noted that fluorescence intensity of protein-immobilized FPSAAN reveals an abrupt climbing when pH is 12.0. The explanation may be that the excessive OH^- in the aqueous solution have a significant effect on the three-dimensional structure and the particle size, causing the rapid hoist of fluorescence intensity. From the Fig. 5, additionally, we can get that the stability of FPSAAN related to pH is significantly higher than that of pure fluorescein. It may be explained by the fact that fluorescein has been embedded into nanoparticles, and the matrix of nanoparticles can protect the embedded fluorophores from effect of pH, thus stabilize the fluorescence emission signal [20]. As a whole, the effect of pH of these nanoparticles is subtle. Therefore, for convenience, we keep the pH fixed at 7.0 in our sequent experiments.

3.2.2 The effect of ionic strength

The effects of ionic strength adjusted with NaCl (ranging from 0.04 to 0.5 mol l^{-1}) of FPSAAN, hydrazide-FPSAAN and protein-immobilized FPSAAN on fluorescent characteristics are illustrated in Fig. 6. It is noted that the fluorescence intensity has a slight change, which mainly caused by the scattering effect. The results indicate that ionic strength exerts a slight effect on fluorescent characteristics of these nanoparticles. The dissimilarities of the fluorescence intensity among different nanoparticles are probably caused by their intermolecular interactions and different surface functional groups, further indicating that FPSAAN modified with functional groups have a great stability.

3.2.3 The effect of time

The effect of time on fluorescent intensity has also been investigated in Fig. 7. When the concentration of FPSAAN was 5.0×10^{-3} g l^{-1}, the fluorescence emission intensity is gradually "quenched" against time (form 307.1 to 117.6), which directly reveals the high sensitive activity of FPSAAN under the condition of low concentration (5.0×10^{-3} g l^{-1}). On the other hand, for hydrazide-FPSAAN and protein-immobilized FPSAAN only a small reduction (from 31.8 to 31.26) of hydrazide-FPSAAN and a subtle increase of protein-immobilized FPSAAN (from 32.33 to 33.71) are observed. Moreover, there is scarcely any change after 96 h. Such phenomena have implied that fluorescence of hydrazide-FPSAAN and protein-immobilized FPSAAN against time have a superior stability under the neutral conditions, which reveals their great potential use in practice.

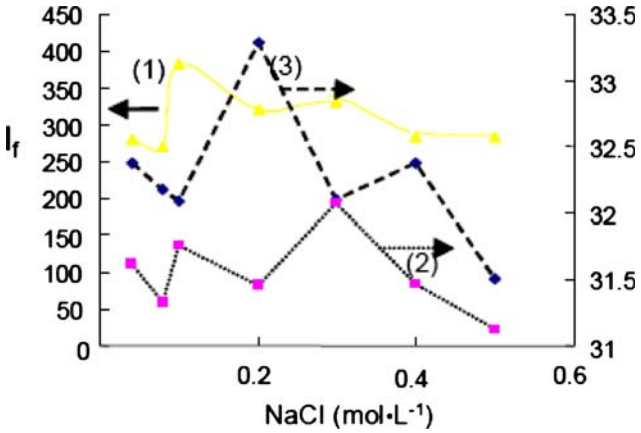

Fig. 6 The effect of ionic strength on fluorescence intensity: FPSAAN (1), hydrazide-FPSAAN (2) and protein-immobilized FPSAAN (3). Concentration of FPSAAN, hydrazide-FPSAAN, or protein-immobilized FPSAAN is 5.0×10^{-3} g L^{-1}(pH 7.0)

3.3 Linear correlation between nanoparticles concentrations and fluorescence intensity

Figure 8 illustrates the change of fluorescence intensity upon the FPSAAN, hydrazide-FPSAAN, and protein-immobilized FPSAAN concentrations, respectively. It can be seen that fluorescence intensity demonstrates a steady and rising trend at lower concentrations, which may be explained by the scattering effect of colloidal particles. However, when the protein-immobilized FPSAAN (FPSAAN or hydrazide-FPSAAN) concentration is higher than 100.0×10^{-3} g l^{-1}(data not shown), the fluorescence

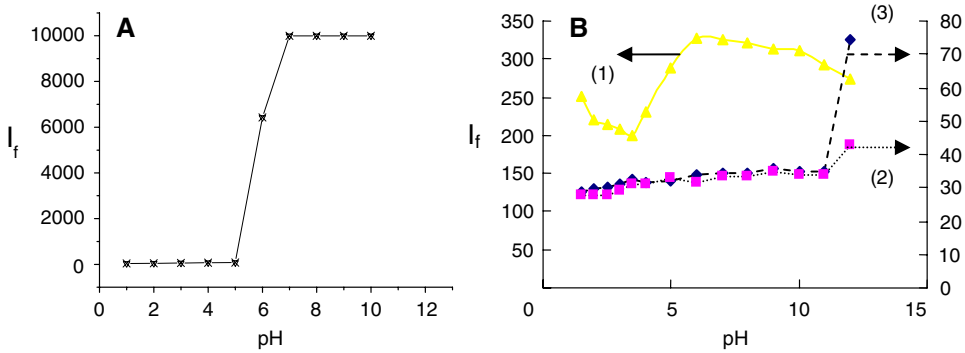

Fig. 5 The effect of pH on fluorescence intensity: **a** fluorescein (excited at 489 nm), and **b** comparison of FPSAAN (1), hydrazide-FPSAAN (2) and protein-immobilized FPSAAN (3). Concentration of FPSAAN, hydrazide-FPSAAN, or protein-immobilized FPSAAN is 5.0×10^{-3} g L^{-1}

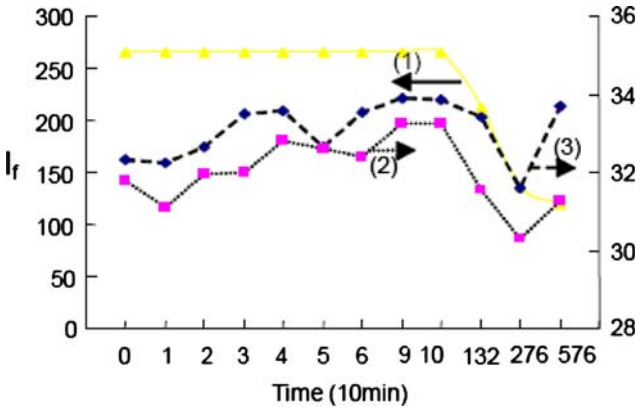

Fig. 7 Fluorescence intensity change against discontinuous time: FPSAAN (1), hydrazide-FPSAAN (2) and protein-immobilized FPSAAN (3). Concentration of FPSAAN, hydrazide-FPSAAN, or protein-immobilized FPSAAN is 5.0×10^{-3} g L^{-1}(pH 7.0)

intensity begins to decrease. We suspect that not only the enhancing intensity of molecular collision quenching but also the decreased intensity of the incident light, which is due to the strong light scattering that could appreciably increase at higher concentrations when a potential secondary aggregation can take place, are accountable for the fluorescence intensity decrease.

Additionally, the fluorescence intensity is proportional to the concentration of nanoparticles in the range of 1.0–100.0 mg l^{-1}. With regard to FPSAAN, the linear regression equation is $y = 52.808x + 16.465$ ($R^2 = 0.9927$) and relative standard deviation is less than 2.0%. As for hydrazide-FPSAAN, the linear regression equation is $y = 5.1814x + 4.1535$ ($R^2 = 0.9935$) and relative standard deviation is below 2.1%. When it comes to protein-immobilized FPSAAN, the linear equation is $y = 5.2227x + 5.2883$. The correlation coefficient is 0.9937 and relative standard deviation is below 3.0%. The results suggest that fluorescence intensity has an excellent linear relation with the FPSAAN (hydrazide-FPSAAN or protein-immobilized FPSAAN) concentrations, which implies their great values in the realm of quantitative detection. Furthermore, in light of the fact that the fluorescence intensity still has a finely linear relation with the concentration after immobilization of BSA on the azidocarbonyl FPSAAN, in all likelihood, it can be applied equally to other proteins such as antibody or antigen. This scenario, if true, would significantly contribute to the potential that azidocarbonyl FPSAAN would be directly used in the field of clinical diagnosis with the superior sensitivity, low cost, and significant reduction of reaction time.

Currently, a lot of biomedical applications have emerged for nanoparticles. The combination of the nanometer size with fluorescent properties leads to their use in labeling as diagnostic tools. Among fluorescent nanoparticles available, nanoparticles with core-shell architecture

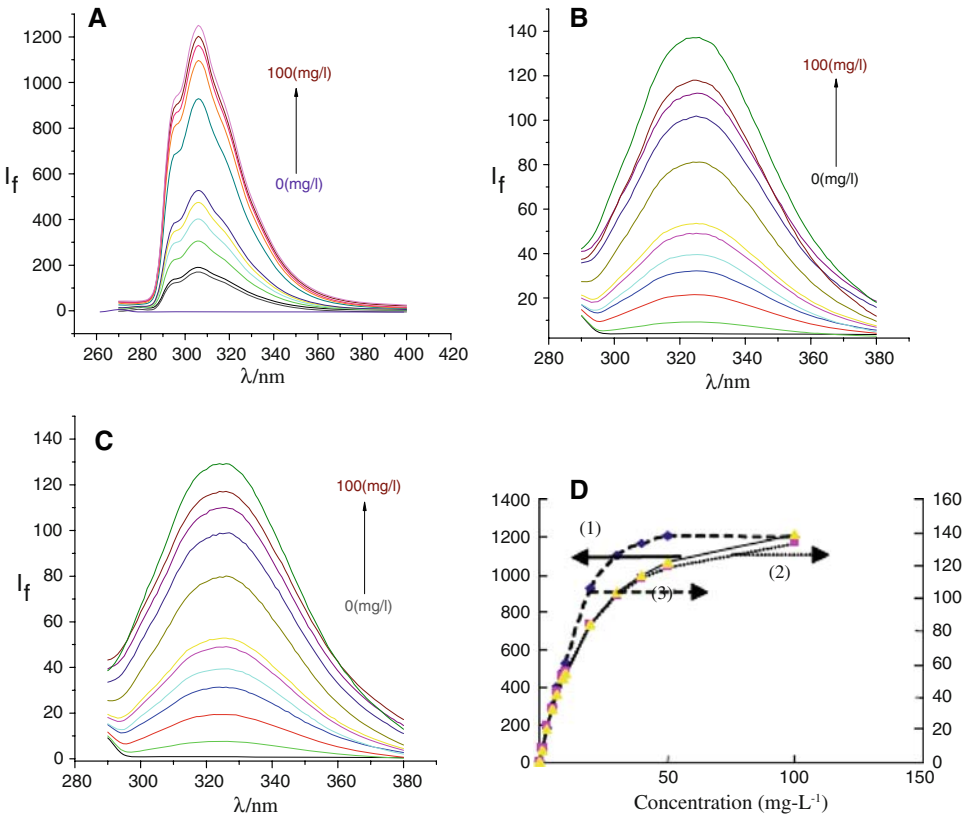

Fig. 8 Fluorescence intensity change upon the concentration (pH 7.0): **a** FPSAAN excited at 253 nm, **b** hydrazide-FPSAAN excited at 260 nm, **c** protein-immobilized FPSAAN excited at 258 nm, and **d** comparison of FPSAAN(1), hydrazide-FPSAAN(2) and protein-immobilized FPSAAN(3)

own the advantages of monodisperse, photostability, and amenable to further surface modification [28, 29]. Magnetic-fluorescent nanoparticles are appealing by reason for their fluorescent and magnetic properties [30]. Although nanoparticles have been proposed as diagnostic tools in many papers, the quantitative measurement based on the fluorescence intensity is rarely mentioned. In our study, FPSAAN not only have the advantages of stable fluorescent characteristics and amenable to further surface modification, but also have linear relation between the fluorescence intensity and nanoparticles concentrations.

3.4 Immobilization of BSA onto azidocarbonyl FPSAAN

As we know, there are two main ways to immobilize protein (enzyme, antibody) on supports, physical adsorption and covalent immobilization. Physical adsorption has the advantages of simplicity and flexibility along with the disadvantages of their weak stability and low protein immobilization capacity. As compared to physical adsorption, covalent immobilization can not only eliminate or significantly reduce leakage of proteins through increased bond strength, but also increase the stability and control of protein binding site availability. However, covalent immobilization requires the supports have functional groups suitable for coupling. Presently, there is considerable interest in the design of protein carriers for practical purposes. From the viewpoint of polymeric materials for protein supports, polymeric materials with hydroxyl, amine, carboxyl and aldehyde groups (–OH, –NH_2, –COOH, –CHO, etc.) [31–34] have been reported in the literature and some of them have been used for protein covalent immobilization. Among them, the instability of aldehyde groups, the low reactivity of hydroxyl groups and the need of cross-linking agent of carboxyl groups limit their wide applications to some extent. Comparatively, the amine groups have a very high stability and reactivity. Moreover, they can be easily modified into azidocarbonyl groups which have higher reactivity and can rapidly react on proteins under mild condition without any cross-linking agent.

In our work, BSA was selected as a model protein to be immobilized onto azidocarbonyl FPSAAN by conjugating the functional azidocarbonyl groups of azidocarbonyl FPSAAN with the free active surface amino groups of BSA under mild condition. To quantify the amount of BSA immobilized on the surface of azidocarbonyl FPSAAN, we used a simple and rapid method based on the difference between the protein content in the starting solution and that remained unbound. The optimized experimental results show that when the initial amount of BSA was 7.0 mg, about 2.88 mg BSA was coupled with azidocarbonyl FPSAAN. It is suggested that azidocarbonyl FPSAAN were heavily coated by BSA at the rate of 41.1%, which exhibits that the useful surface functional groups of FPSAAN have a high reactivity and can rapidly covalently combined with proteins with a superior immobilization capacity.

3.5 Influence of the hCG antigen and plasma

Before the hCG antigen and plasma were added, the fluorescent characteristics of hCG antibody immobilized FPSAAN were measured. The results, shown in Fig. 9a and b, demonstrate that fluorescence intensity of hydrazide-FPSAAN decreases after the immobilization of hCG antibody onto azidocarbonyl FPSAAN. This is probably attributable to the scatting effects and surface groups just as the discussions above (3.2 Fluorescent characteristics). Additionally, hCG antibody immobilized FPSAAN have the similar fluorescent characteristics to BSA immobilized FPSAAN. The maximum excitation and emission wavelengths are consistent with those of BSA immobilized FPSAAN. Only negligible difference of fluorescence intensity can be found.

In order to investigate the influence of hCG antigen and human plasma on the fluorescent characteristics of hCG antibody immobilized FPSAAN, we also measured the fluorescent characteristics after the hCG antigen and human plasma were added. As shown in Fig. 9b and c, the fluorescent spectra and intensity almost remain the same after binding with the hCG antigen, which further reflects the stable fluorescent characteristics of immobilized FPSAAN. Similarly, the fluorescent characteristics of hCG antibody immobilized FPSAAN are not obviously affected

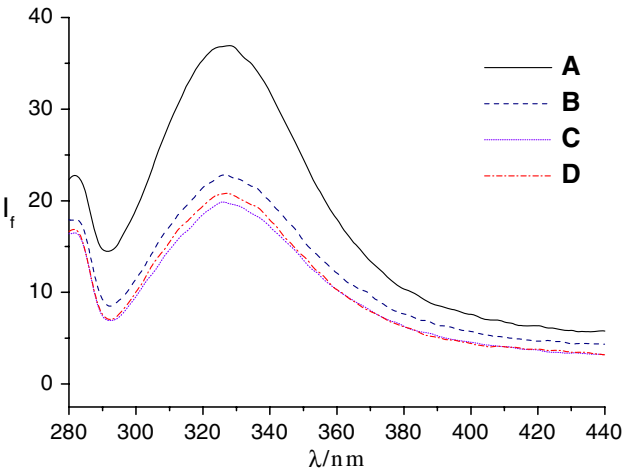

Fig. 9 Fluorescence spectra of A hydrazide-FPSAAN, B hCG antibody immobilized FPSAAN, C human plasma-hCG antibody immobilized FPSAAN and D hCG antigen-hCG antibody immobilized FPSAAN

after human plasma was added (shown in Fig. 9b, d). Above results suggest that immobilized FPSAAN can be used as a diagnostic tool in the clinical study on the basis of their stable fluorescence.

4 Conclusions

In this paper, nanometer-size functionalized FPSAAN with azidocarbonyl groups, narrow size distribution and sensitive fluorescent properties were synthesized by means of soapless emulsion polymerization method. Fluorescein was selected as fluorescent reporter, azidocarbonyl groups were fabricated on the surface of FPSAAN and BSA was used as a model protein to be covalently immobilized on azidocarbonyl FPSAAN. Meanwhile, the hCG antibody was also immobilized on azidocarbonyl FPSAAN. Afterwards, the hCG antigen as well as human plasma was mixed with them to evaluate the possible changes of fluorescence. The results show that FPSAAN possess the preferred monodispersed nano-sized property and stable fluorescent characteristics. In addition, azidocarbonyl FPSAAN fabricated by hydrazinolysis and azido-reaction have a strong coupling reactivity with proteins. Remarkably, fluorescence intensity has an excellent linear relation with the nanoparticles concentration. The benefits of the finely linear relationship transcend mere qualitative detection, for the large quantities of fluorescent tracer which may be borne by the carrier material permit increased sensitivity and thus completely automated, quantitative, photoelectric measurement and monitoring.

Acknowledgments This study has been supported by grants from National Natural Science Foundations of China (Nos. 30772658 and 30570494).

References

1. M. Tabuchi, M. Ueda, N. Kaji, Y. Yamasaki, Y. Nagasaki, K. Yoshikawa, K. Kataoka, Y. Baba, Nat. Biotechnol. **22**, 337–340 (2004). doi:10.1038/nbt939
2. X.Q. Liu, Y.P. Guang, H.Z. Liu, Z.Y. Ma, Y. Yang, X.B. Wu, J. Magn. Magn. Mater. **293**, 111–118 (2005). doi:10.1016/j.jmmm.2005.01.051
3. Y. Weizmann, F. Patolsky, E. Katz, I. Willner, J. Am. Chem. Soc. **125**, 3452–3454 (2003). doi:10.1021/ja028850x
4. M. Nichkova, D. Dosev, S.J. Gee, B.D. Hammock, I.M. Kennedy, Anal. Chem. **77**, 6864–6873 (2005). doi:10.1021/ac050826p
5. B.N.G. Giepmans, S.R. Adams, M.H. Ellisman, R.Y. Tsien, Science **312**, 217–223 (2006). doi:10.1126/science.1124618
6. Y.R. Duan, Q. Wang, Z.R. Zhang, J. Mater. Sci: Mater. Med. **17**, 509–516 (2006). doi:10.1007/s10856-006-8933-3
7. Z.Q. Wu, S.L. Gong, C. Li, Z. Zhang, W.H. Huang, L.Z. Meng, X.J. Lu, Y.B. He, Eur. Polym. J. **41**, 1985–1992 (2005). doi:10.1016/j.eurpolymj.2005.03.021
8. L. Josephson, M.F. Kircher, U. Mahmood, Y. Tang, R. Weissleder, Bioconjug. Chem. **13**, 554–560 (2002). doi:10.1021/bc015555d
9. H. Ow, D.R. Larson, M. Srivastava, B.A. Baird, W.W. Webb, U. Wiesner, Nano. Lett. **5**, 113–117 (2005). doi:10.1021/nl0482478
10. J.F. Peng, K.M. Wang, W.H. Tan, X.X. He, C.M. He, P. Wu, F. Liu, Talanta **71**, 833–840 (2007). doi:10.1016/j.talanta.2006.05.064
11. J. Choi, Y. Zhao, D. Zhang, S. Chien, Y.H. Lo, Nano. Lett. **3**, 995–1000 (2003). doi:10.1021/nl034106e
12. H.L. Jiang, K.J. Zhu, Biomaterials **23**, 2345–2351 (2002). doi:10.1016/S0142-9612(01)00368-4
13. S.A. Kushon, K.D. Ley, K. Bradford, R.M. Jones, D. McBranch, D. Whitten, Langmuir **18**, 7245–7249 (2002). doi:10.1021/la026211u
14. B.I. Lemon, R.M. Crooks, J. Am. Chem. Soc. **122**, 12886–12887 (2000). doi:10.1021/ja0031321
15. C.S. Yang, C.H. Chang, P.J. Tsai, W.Y. Chen, F.G. Tseng, L.W. Lo, Anal. Chem. **76**, 4465–4471 (2004). doi:10.1021/ac035491v
16. S. Santra, P. Zhang, K. Wang, R. Tapec, W. Tan, Anal. Chem. **73**, 4988–4993 (2001). doi:10.1021/ac010406+
17. C. Wu, C. Szymanski, J. McNeill, Langmuir **22**, 2956–2960 (2006). doi:10.1021/la060188l
18. B. Dubertret, P. Skourides, D.J. Norris, V. Noireaux, A.H. Brivanlou, A. Libchaber, Science **298**, 1759–1762 (2002). doi:10.1126/science.1077194
19. C.R. Goldsmith, J. Jaworski, M. Sheng, S.J.J. Lippard, J. Am. Chem. Soc. **128**, 418–419 (2006). doi:10.1021/ja0559754
20. J.W. Gratama, J.L. D'Hautcourt, F. Mandy, G. Rothe, D. Barnett, G. Janossy, S. Papa, G. Schmitz, R. Lenkei, Cytometry **33**, 166–178 (1998). doi:10.1002/(SICI)1097-0320(19981001)33:2<166::AID-CYTO11>3.0.CO;2-S
21. C. Scholz, M. Iijima, Y. Nagasaki, K. Kataoka, Macromolecules **28**, 7295–7297 (1995). doi:10.1021/ma00125a040
22. S.E. Shim, H. Lee, S. Choe, Macromolecules **37**, 5565–5571 (2004). doi:10.1021/ma049930j
23. W.H. Tan, K.M. Wang, X.X. He, X.J. Zhao, T. Drake, L. Wang, R.P. Bagwe, Med. Res. Rev. **24**, 621–638 (2004)
24. Z.Y. Ma, Y.P. Guan, X.Q. Liu, H.Z. Liu, Polym. Adv. Technol. **16**, 554–558 (2005). doi:10.1002/pat.618
25. Y.C. Liu, G.J. Dong, Y.C. Zhao, J. Immunol. Methods **124**, 159–163 (1989). doi:10.1016/0022-1759(89)90348-7
26. G.P. Wang, E.Q. Song, H.Y. Xie, Z.L. Zhang, Z.Q. Tian, C. Zuo, D.W. Pang, D.C. Wu, Y.B. Shi, Chem. Commun. **34**, 4276–4278 (2005)
27. W. Mehnert, K. Mäder, Adv. Drug Deliv. Rev. **47**, 165–196 (2001). doi:10.1016/S0169-409X(01)00105-3
28. K. Aslan, M. Wu, J.R. Lakowicz, C.D. Geddes, J. Am. Chem. Soc. **129**, 1524–1525 (2007). doi:10.1021/ja0680820
29. J.E. Fuller, G.T. Zugates, L.S. Ferreira, H.S. Ow, N.N. Nguyen, U.B. Wiesner, R.S. Langer, Biomaterials **29**, 1526–1532 (2008). doi:10.1016/j.biomaterials.2007.11.025
30. F. Bertorelle, C. Wilhelm, J. Roger, F. Gazeau, C. Me'nager, V. Cabuil, Langmuir **22**, 5385–5391 (2006). doi:10.1021/la052710u
31. T.M. Blattler, S. Pasche, M. Textor, H.J. Griesser, Langmuir **22**, 5760–5769 (2006). doi:10.1021/la0602766
32. C.D. Hahn, C. Leitner, T. Weinbrenner, R. Schlapak, A. Tinazli, R. Tampe, B. Lackner, C. Steindl, P. Hinterdorfer, H.J. Gruber, M. Holzl, Bioconjug. Chem. **18**, 247–253 (2007). doi:10.1021/bc060292e
33. C.H. Ho, L. Limberis, K.D. Caldwell, R.J. Stewart, Langmuir **14**, 3889–3894 (1998). doi:10.1021/la980148k
34. S. Ko, J. Jang, Biomacromolecules **8**, 1400–1403 (2007). doi:10.1021/bm070077g